Reprinted from:

EARTH AND PLANETARY SCIENCE LETTERS

A LETTER JOURNAL DEVOTED TO THE DEVELOPMENT IN TIME OF THE EARTH AND PLANETARY SYSTEM

Volume 19, No. 1, May 1973

EXPERIMENTAL MELTING STUDIES ON A MODEL UPPER MANTLE COMPOSITION AT HIGH PRESSURE UNDER WATER-SATURATED AND WATER-UNDERSATURATED CONDITIONS

D.H. GREEN

Dept. of Geophysics and Geochemistry, Australian National University, Canberra, Australia

pp. 37–53

NORTH-HOLLAND PUBLISHING COMPANY - AMSTERDAM.

EARTH AND PLANETARY SCIENCE LETTERS 19 (1973) 37–53. NORTH-HOLLAND PUBLISHING COMPANY

EXPERIMENTAL MELTING STUDIES ON A MODEL UPPER MANTLE COMPOSITION AT HIGH PRESSURE UNDER WATER-SATURATED AND WATER-UNDERSATURATED CONDITIONS

D.H. GREEN
Dept. of Geophysics and Geochemistry, Australian National University, Canberra, Australia

Received 3 January 1973
Revised version received 5 March 1973

The solidus of a model pyrolite composition is sensitively dependent on water content and has been determined experimentally up to 40 kb, for water-saturated (6% H_2O) and water-undersaturated (0.2% H_2O) conditions. Pargasitic hornblende is a major subsolidus phase to 29 kb and its breakdown at higher pressure has the effect of sharply depressing the solidus for (pyrolite + 0.2% H_2O) from ~1150°C to ~1020°C between 25 and 29 kb. Experiments have been carried out above the solidus to determine the nature of the partial melting process, particularly the nature and composition of the residual phases at a specific pressure, temperature and water content. The presence of siliceous (>58% SiO_2), low-magnesium glasses, broadly of andesitic or dacitic character, in experiments quenched at both 10 kb and 20 kb, is shown to be due to growth during quenching of olivine, clinopyroxene, amphibole and mica. However, it is possible in some experiments to use the compositions of the starting mix and analyzed residual phases to calculate the composition of the *equilibrium liquid* and degree of melting at the particular condition. High degrees of melting under water-saturated conditions at *10 kb* yield magnesian, quartz-normative basaltic andesites ~10% Qz, (1100°C, 28% melting) to quartz tholeiite magmas 5–7% Qz, (1200°C, 32.5% melting), and at *20 kb*, yield olivine tholeiite magmas (1100°C, 27–30% melting). Andesitic or dacitic magmas are not products of equilibrium partial melting of pyrolite at $P > 10$ kb under water-saturated conditions but may be derived from parental olivine-poor tholeiites, quartz tholeiites or basaltic andesites ($P < 10$ kb) by crystal fractionation. Parental magmas of the island arc tholeiitic magma series may originate by partial melting of upper mantle peridotite (pyrolite or residual peridotite of the lithosphere) under water-saturated conditions at ~5–20 kb.

1. Introduction

In a recent paper, Kushiro et al. [1] report the results of experimental melting [7] of a peridotitic composition (lherzolite inclusions from Salt Lake Crater, Hawaii) at 20 kb and 26 kb under water-saturated conditions (30% H_2O). With high degrees of melting (~20%), glass was obtained among the run products, together with olivine, orthopyroxene and clinopyroxene. The compositions of the latter phases were quite different from those of the starting material, providing evidence that reaction to a new equilibrium assemblage has occurred under the experimental conditions. The composition of the glass, analyzed by electron microprobe, was high in SiO_2, Al_2O_3 and CaO and also apparently contained ~13% H_2O. The authors noted that their glass composition was broadly andesitic or dacitic in character and not basaltic. These experimental data were thus taken to support models of direct derivation of siliceous magmas (>55% SiO_2) by partial melting of mantle peridotite under water-saturated conditions [1, 8, 9].

In this laboratory, melting experiments on a model pyrolite composition under water-saturated conditions yielded very similar data to those described above. However, it can be shown that the glass obtained is metastable, with a composition determined by growth of quench amphibole, mica olivine and pyroxene, and does not correspond to the composition of a liquid in equilibrium with olivine, orthopyroxene and clinopyroxene. The data presented in this paper support and are complementary to studies by Nicholls and Ringwood

[2] which have shown that quartz-normative liquids (including quartz tholeiite, andesite, dacite) do not have olivine as a liquidus phase at pressures > 20 kb, even for water-saturated conditions, and thus cannot be direct partial melts of a peridotitic source rock.

2. Experimental methods

Experiments were carried out in a piston-cylinder apparatus using welded $Ag_{75}Pd_{25}$ and $Ag_{50}Pd_{50}$ sample capsules containing known quantities of water. The composition investigated was a model pyrolite [4] as shown in analysis 1, table 1. To diminish the dominance of olivine and consequent high proportions of crystals to liquid under conditions of partial melting, a composition equivalent to pyrolite minus 40% olivine ($Mg_{91.6}Fe_{8.1}Mn_{0.1}Ni_{0.2}$) was used in all experiments [5, 6]. Sample weights of 15 mg were used with a water content of 10%. The water was added by microsyringe and checked by weighing before and after welding. With such a large water content, piercing of the capsule after the run yielded small droplets of water and drying of the opened sample at 110°C showed that 7–9% water was 'free' after quenching of the sample. These techniques also readily identified any runs in which capsule failure has caused loss of water.

TABLE 1
Compositions of pyrolite [16] and pyrolite minus 40% olivine (Olivine of composition $Mg_{91.6}Fe_{8.1}Ni_{0.2}Mn_{0.1}$). The latter composition is that used in experimental runs

	Pyrolite	Pyrolite minus 40% olivine	Spinel lherzolite Kushiro et al. [1, 7]
SiO_2	45.2	47.8	48.3
TiO_2	0.7	1.2	0.2
Al_2O_3	3.5	5.9	4.9
Fe_2O_3	0.5	0.8	–
FeO	8.0	8.2	10.0
MnO	0.1	0.1	0.1
MgO	37.5	28.7	32.5
CaO	3.1	5.1	3.0
Na_2O	0.6	0.95	0.7
K_2O	0.13	0.22	0.07
P_2O_5	–	–	–
Cr_2O_3	0.4	0.7	0.3
NiO	0.2	0.2	–
$\frac{100Mg}{Mg + Fe^{++}}$	89.2	86.5	85.2
$\frac{100Mg}{Mg + \Sigma Fe}$	88.9	85.2	85.2

As there is > 10% olivine present in all experiments reported in this paper, the water content of 10% added to the olivine-depleted pyrolite is equivalent to an experimental study of standard pyrolite with 6% water added. In addition to experiments with excess water, the pyrolite solidus and melting relationships for $p_{H_2O} < P_{total}$ were determined using a composition (pyrolite minus 40% olivine plus 0.3% H_2O) equivalent to (pyrolite plus 0.2% H_2O). In studying the water-undersaturated melting relationships in pyrolite it is necessary to add accurately the very small quantities of water. To overcome the weighing error and practical difficulty of weighing or micropipetting 0.03 mg H_2O to a 10 mg sample, large capacity runs [100 mg (pyrolite minus 40% olivine) + 0.3 mg H_2O] were carried out at 15 kb, 1000°C for 6 hr. This produced fine-grained assemblages of olivine + amphibole + pyroxenes in which the water is locked in amphibole. This material was finely ground and mixed, and 10 mg portions were re-run under various P, T conditions using sealed $Ag_{75}Pd_{25}$ Ag_{50},Pd_{50} or Pt capsules (Pt at $T > 1250$°C at 30 kb or $T > 1150$°C at 5 kb). The experimental method is equivalent to a study of pyrolite + 0.2% H_2O, or, in mineralogical terms, of hornblende peridotite containing 15–20% pargasitic hornblende (compared with a maximum pargasitic hornblende content of about 30% for pyrolite composition [12] with excess water and subsolidus conditions at about 10 kb).

Experimental charges were examined microscopically in transmitted light and polished mounts were also prepared. The latter method enabled close observation of the textures of melting and subsolidus runs, the recognition of glass by its low reflectivity and interstitial habit, the distinction between quench and primary phlogopite, and the recognition of abundant and evenly distributed gas-phase bubbles. Solid phases were analyzed using an electron microprobe and non-dispersive X-ray analytical system, based on the TPD microprobe [10]. Full details of the instrument and analytical procedures will be described elsewhere by Reed and Ware [30]. Conditions of analyses are as described previously [11] but several features of this instrument are particularly important for the present investigation. Firstly, the specimen current of 3–5 nA is an order of magnitude lower than that for most electron microprobe systems but in spite of this, careful investigation by I.A. Nicholls showed that highly siliceous and water-rich glasses suffered specimen damage and Na-volatilization by the electron beam during 100 sec analysis-time at each point. Thus the analyses of glass were carried out, where possible, by continuously moving the beam on an area of glass or by counting for 10 sec on each of 10 glass spots. This resulted in an increase of apparent Na content from ~ 0.5% to 1.5% Na_2O but it is recognized that these figures may still be low. It was possible to analyze simultaneously for Na, Mg, Si, P, Kt, Ca, Ti, Cr, Mn, Fe at each point and this permitted the identification and analysis of quench amphibole and quench clinopyroxene, as well as primary phases. The analytical method also identified real compositional variations within the glass, although for such "point" analyses, Na-figures are not reliable. In the TPD instrument the high quality optics and ability to view the sample while

TABLE 2

	Most Fe-rich olivine core of larger crystals *	Most common olivine, cores of small crystals *	Quench border; average of ~1–2 μ rim *	Calculated equilibrium olivine, no Fe-loss *	Chromite included in olivine	Glass Average **	Glass range ** (7 analyses)	Bulk composition of sample after experiment†	Calculated equilibrium liquid. Starting composition minus [45% olivine ($Fo_{90.1}$) + 1% chromite]
	1	2	3	4	5	6	7	8	9
SiO_2	41.3	41.2	39.8	40.9	–	59.7	59.2 – 60.2	49.2	54.6
TiO_2	–	–	–	–	3.0	2.5	2.5 – 2.7	1.1	2.2
Al_2O_3	–	–	0.6	–	10.0	13.7	13.2 – 14.1	6.1	10.7
Fe_2O_3	–	–	–	–	–	–	–	–	1.5
FeO	8.2	6.8	14.5	9.7	14.0	4.6	4.4 – 4.8	6.2	6.9
MnO	–	–	–	0.1	–	–	–	0.1	0.2
MgO	50.4	52.0	45.9	49.3	9.0	4.6	3.9 – 5.3	30.1	11.9
CaO	0.1	0.1	–	0.1	–	12.7	12.4 – 13.1	5.4	9.4
Na_2O	–	–	–	–	–	1.4	1.1 – 1.6	0.8	1.9
K_2O	–	–	–	–	–	0.6	0.6	0.2	0.4
Cr_2O_3	–	–	–	–	64.0	0.4	0.2 – 1.4	0.7	0.1
P_2O_5	–	–	–	–	–	0.2	00.2– 0.3	–	–
(H_2O)	–	–	–	–	–	(11%	–	–	–
$\frac{100\ Mg}{Mg + \Sigma Fe}$	91.6	93.0	84.5	–	52	64	61 – 66	89.7	72
$\frac{100\ Mg}{Mg + Fe^{++}}$	91.6	93.0	84.5	90.1	–	–	–	–	75.5

Run conditions: 10 kb, 1200°C, 1 hr, $Ag_{50}Pd_{50}$ capsule. 100 Mg/(Mg + ΣFe) of sample after run: 89.7.

* Some large (~30 μ) olivine crystals show reverse zoning reflecting growth of the crystal prior to Fe-loss to the $Ag_{50}Pd_{50}$ capsule (column 8) and failure of the centres of crystals to readjust to equilibrium as the bulk composition changed. Outer parts of such crystals and centres of smaller (10 μ) crystals have compositions Fo_{93} (column 2) and are taken to be in equilibrium in the bulk composition of column 8. Analyses of the outermost 1–2 μ of crystals, after correction for partial admixture of glass and high TiO_2 (quench ilmenite?) in the analysed volume, show compositions averaging $Fo_{84.5}$, indicating the presence of thin shells of olivine quench outgrowth on the primary crystals (column 3).

** The glass composition was obtained using only data from analyses in which the electron beam was moved over the areas of glass during analysis (100 sec). Data from stationary beam analyses, when corrected for low Na values, yield an almost identical average composition. In this and following tables glass compositions are recalculated to 100% anhydrous. The "H_2O" figure is estimated from the failure of the 11 elements determined to total to 100%, in contrast to totals of 98–101% for olivines and pyroxenes.

† Determined with 30 μ defocussed beam in continuous movement over polished surface of sample.

under the electron beam remove any uncertainty in correlating analytical data with petrographic observation.

To determine the effect of iron loss from the sample to the Ag–Pd capsule, bulk analyses of the samples were carried out using a defocussed (30 μ diameter) electron beam kept in continuous movement over the polished surface of the sample. The resultant analyses (e.g. table 2, column 8) gave excellent agreement with that of the initial mix (table 1, column 2) when corrected for Fe-loss, and thus provided a check on the analytical method. The data showed that there was appreciable iron loss from the 10 kb, 1200°C run (from 100 Mg/(Mg + ΣFe) = 85.2 to 89.7), slight iron loss from the 10 kb, 1100°C run, but no significant loss from 10 kb runs at $T < 1100$°C or in the 20 kb runs at $T \leqslant 1100$°C (see tables 2–12).

3. Experimental results

3.1. Water-saturated solidus

The experimental data are summarized in fig. 1 showing the results applied to pyrolite + 6% H_2O. The solidus is markedly depressed below the anhydrous solidus and is readily distinguished by textural change and the disappearance of phlogopite and amphibole at the beginning of melting at 30 kb and 20 kb respectively. At 10 kb the preferred solidus is shown as a solid line although the presence of rare, very low-R.I. glass and coarser grain size of the 970°C run relative to the 900°C run suggest that the solidus may lie at the lower-temperature dotted line. The glass at 970°C may however be quenched from the excess, intergranular vapour phase. Examination of the polished surface shows this vapour phase to be evenly distributed throughout the charge. Amphibole is an abundant phase in both the 900°C and 970°C runs accompanied by olivine and orthopyroxene and, at 970°C at least, by minor clinopyroxene *. There is no difference in Mg-value of orthopyroxene between the 900°C and 970°C runs so that the amount of melting at 970°C could only be very small. In addition, the Na/K, Ti/Na and Ti/K ratios of the amphibole at 970°C are close to those of the initial mix so that there are no chemical grounds from which to infer the existence of a low-melting fraction enriched in K, or Ti or Na, in addition to the solid phases at 970°C.

* The compositions and approximate proportions of olivine, orthopyroxene and amphibole also show that there should be another phase present in the pyrolite composition, with higher Ca : Al ratio than either orthopyroxene or amphibole.

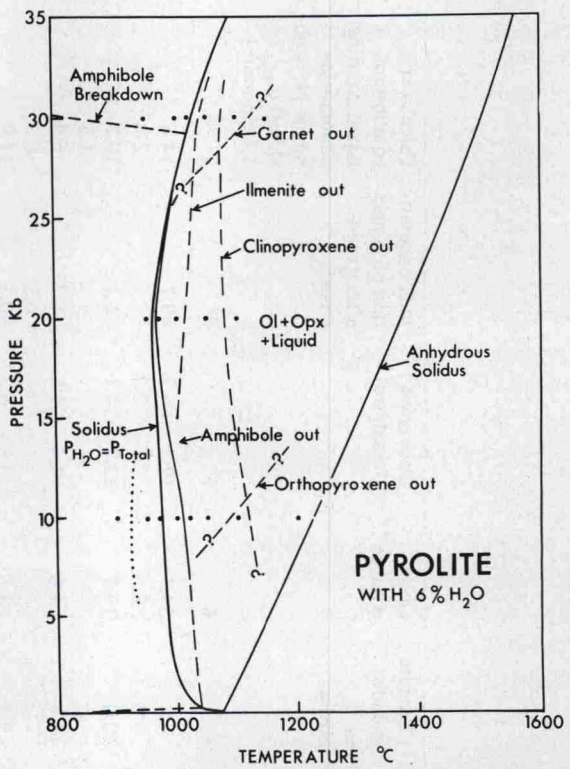

Fig. 1. Experimental determination of the water-saturated solidus for pyrolite composition. Experiments were carried out on (pyrolite minus 40% olivine) composition with 10% water added and data points are shown as black dots in the diagram. The subsolidus mineral assemblage at 10 kb and 20 kb is olivine + orthopyroxene + amphibole + clinopyroxene but at 30 kb the subsolidus assemblage is olivine + orthopyroxene + garnet + clinopyroxene + phlogopite + titanoclinohumite + ilmenite. The disappearance of major phases above the solidus is also shown. The anhydrous solidus is from ref. [6].

There are minor differences between the amphibole, considered to be subsolidus, at 970°C and that at 1000°C, where a minor melt fraction is observed and is considered to have caused the decreased K content and increased Na/K and Ti/Na ratios of the amphibole. The marked difference in Cr_2O_3 content of amphibole between 970°C and 1000°C is probably due to a tiny spinel inclusion in the 970°C amphibole, several other less satisfactory amphibole anlayses having about 1% Cr_2O_3. For the above reasons, the solidus at 10 kb is placed between 970°C and 1000°C and not at the lower-temperature dotted line of fig. 1. The order of disappearance of phases with increasing degree of melting is shown in fig. 1. There are minor

changes from the preliminary diagram previously published [12] and based only on optical examination of crushed samples. Later optical and microprobe examination of polished mounts shows that olivine alone is present as an equilibrium crystalline phase at 10 kb, 1200°C; clinopyroxene and olivine are present at 10 kb, 1100°C and orthopyroxene first appears at 10 kb, 1050°C. The runs at 10 kb, 1000°C and 1020°C contain small euhedral amphibole laths and the crystal habit, textural relations and grain size led to the interpretation that these were primary crystals, in equilibrium with olivine, orthopyroxene and clinopyroxene. However, microprobe analysis of amphibole from runs at 1050°C and 1020°C yielded compositions of silica-rich amphiboles, with low CaO contents and Mg-values * which are much lower than those of the subsolidus amphibole at 970°C or of the coexisting olivine and pyroxenes. On the other hand, the amphibole at 1000°C resembles that at 970°C except for the differences in Na, Ti, and K. The amphiboles at 1050°C and 1020°C are thus either quench amphiboles or largely quench outgrowths of amphibole on small cores of primary amphibole. The amphibole-out curve [13] is placed between 1000°C and 1020°C, i.e. within ~ 40°C of the solidus rather than 60°C above the solidus as shown in the preliminary diagram [12].

Ilmenite is a minor but distinctive phase, persisting to $\geqslant$ 40°C above the solidus at 20 kb but for $<$ 30°C at 30 kb. Garnet is absent at 20 kb but is an important residual phase at 30 kb where it persists ~ 100°C above the solidus, i.e. about 50°C higher than the disappearance of clinopyroxene.

3.2. Water-undersaturated solidus

In addition to experiments on pyrolite + 6% H_2O, a programme of melting and subsolidus experiments applicable to pyrolite + 0.2% H_2O has been completed (fig. 2) and a further study on pyrolite + 1.2% H_2O is in progress. The solidus for $p_{H_2O} < P_{total}$ has a very different shape from that for $p_{H_2O} < P_{total}$ and is determined by the pargasitic hornblende stability field. Colourless, pargasitic hornblende disappears at or very

* The abbreviation Mg-value is used for the atomic ratio 100 Mg/(Mg + ΣFe).

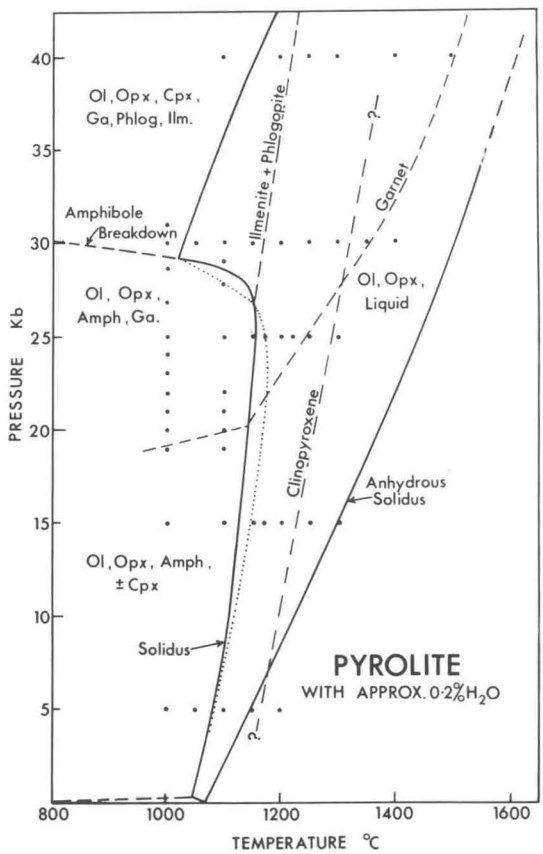

Fig. 2. Experimental determination of solidus for water-undersaturated (at $P < 30$ kb) melting of pyrolite minus 40% olivine and of sub-solidus and above-solidus mineralogy for a water content in pyrolite equivalent to approximately 0.2%. The "dotted" curve shows the position of the solidus deduced [12] from preliminary data on amphibole stability in pyrolite and in the melting interval of undersaturated basaltic compositions. The data points are shown by heavy dots and the minerals present in the subsolidus disappear during melting along the dashed curves marked with the mineral names. Amphibole disappears at the solidus (within the limits of the experimental points) for $P <$ 30 kb.

close to the pyrolite solidus for P $<$ 30 kb and neither ilmenite nor phlogopite are observed either for subsolidus or above-solidus conditions at $P < 27$ kb approximately. Both ilmenite and phlogopite persist however for about 150°C above the solidus at 30 kb and $\geqslant$ 50 – 100°C at 40 kb. Rare garnet appears on the solidus at 20 kb but persists for ~ 350°C above the solidus at 30 kb compared with ~ 100°C above the solidus for $p_{H_2O} = P_{total}$ at 30 kb (fig. 1). Both clinopy-

roxene and orthopyroxene (particularly at 10 kb, figs. 1,2) also persist over a wide temperature range above the solidus. These differences are directly attributable to the much lower degree of melting at a given P_{total} T in pyrolite with low water content. Almost all the partial melting data points of figs. 1 and 2 are below the anhydrous solidus for pyrolite.

4. Melting in the upper mantle

The data of figs. 1 and 2 and that for anhydrous pyrolite [5, 6] provide a firm experimental basis for discussion of melting behaviour in the upper mantle. If the upper mantle is anhydrous then estimates of the geothermal gradient beneath either oceans or continents do not intersect the pyrolite solidus. If, however, there is a small water content ($< 0.4\%$ approximately) in an upper mantle of pyrolite composition the solidus for $p_{H_2O} < P_{total}$ between 27 and 29 kb produces a situation where a geothermal gradient may pass from subsolidus to above-solidus conditions at depths of ~ 90 km [6, 12 – 15]. The existence of the low velocity zone (LVZ), particularly in oceanic crustal regions, is considered to be a direct result of the intersection of a normal geothermal gradient with the pyrolite solidus for $p_{H_2O} < P_{total}$. The depth of the "roof" of the LVZ, defined by the intersection of geotherm and pyrolite solidus, is relatively insensitive to changes in temperature over a 100°C temperature range or in changes in water content from nearly anhydrous up to about 0.4%. Changes in these parameters in the mantle will, however, affect the degree of partial melting [12, 15] and thus the seismic velocities and attenuation *within* the LVZ. If the geothermal gradient is very low then it may not intersect the pyrolite solidus at all (LVZ absent and lithosphere "welded" to upper mantle) or may intersect the solidus at $P > 30$ kb to produce extremely small degrees of melting and a deep low-velocity zone. If the geothermal gradient is very steep then melting may begin at < 27 kb and the degree of melting within the LVZ will be proportionately large. This situation would probably be very unstable and diapirism and magmatism from the LVZ would occur.

The possibility of addition of water to the low velocity zone, by dehydration of lithosphere beneath a neighbouring Benioff zone [2, 3, 12, 14, 18, 19] or by upward concentration of water-rich fluid or magma within the LVZ [17], would initially lead to formation of increasing amounts of amphibole in the "roof" (lithosphere). However this can only absorb up to about 0.4% H_2O [12, fig. 3] – higher water contents would produce conditions of $p_{H_2O} = P_{total}$ and the relevant solidus would be that of fig. 1. It is thus possible, without changing the local geothermal gradient, for the depth to the top of the LVZ to change rather abruptly from ~90 km to ~65 km by addition of small quantities of water [12, 13]. The amount of melt formed along the geothermal gradient would again be very sensitively controlled by the amount of water present [12]. It is suggested that melting of mantle peridotite under water-saturated conditions occurs beneath island arcs, caused by access of water from dehydration reactions occurring within the subducted crust and lithosphere of the downgoing slab. Thus the solidus of fig. 1 is relevant to the island arc situation leading to partial melting at very shallow depths along normal geothermal gradients in the upper mantle. Melting due to water access may occur in parts of the mantle that, prior to initiation of the downgoing slab, comprised the lithosphere overlying the LVZ. The latter feature may account for some of the puzzling features of the island arc tholeiitic and basaltic andesite magmas, particularly the observations that TiO_2, Na_2O, rare-earth elements and other incompatible elements are present in *lower* abundance than in mid-ocean ridge tholeiites, of similar or more magnesian major element composition or even of less fractionated composition [18, 20]. If the oceanic lithosphere is formed at a mid-oceanic ridge, then the peridotite forming the lithosphere must be partially residual in character and depleted in incompatible elements relative to the primary mantle material which, in upwelling at the mid-oceanic ridges, gave rise to basaltic oceanic crust and residual peridotite lithosphere. If, in its later history, a region of depleted lithosphere is remelted above a "subduction zone", then the products of melting will have their major element chemistry determined by equilibria involving olivine and pyroxene but their incompatible element contents will reflect the residual and depleted character of the "reactivated lithosphere".

5. Chemical compositions of liquids formed by equilibrium partial melting of pyrolite under water-saturated conditions

5.1. Compositions of quenched glasses and equilibrium liquids in experimental runs at 10 kb

5.1.1. 10 kb, 1200°C

The experimental run at 10 kb, 1200°C showed excellent partial melting texture with euhedral olivines (~50%) and uncommon, small chromite crystals in glass. No evidence for quench amphibole or clinopyroxene was found by either optical or X-ray powder diffraction examination. Because of the simplicity of the run products it is possible to deduce a great deal about both the equilibrium partial melting of pyrolite at 10 kb and 1200°C under water-saturated conditions, and about the nature of the quenching process in recovering the sample for petrographic study. While the optical, microprobe and X-ray diffraction identification of quench amphibole and clinopyroxene in lower temperature runs at 10 kb and in runs at 20 kb casts immediate doubt on the glass compositions as those of an equilibrium liquid, this does not obviously apply to the 10 kb, 1200°C and 10 kb, 1100°C runs. Thus these two runs were examined in detail as test cases to establish whether the nature of liquids derived by partial melting of peridotite could be directly determined from the composition of quenched glasses.

Analyses of glass using both stationary beam (giving low Na_2O values of 0.4% due to volatilization) and with the electron beam kept continually in motion during analysis within larger "pools" of glass (giving higher Na_2O values of 1.4% but very similar values for other elements) showed that the glass is of high SiO_2 and Ca, and low Mg and Fe character. The glass is strongly quartz normative (20%) and could be broadly classed as andesitic. However the compositions given in tables 1 and 2 show that it is not possible to obtain a mass balance for the original bulk composition of the charge (table 1) if magnesian olivine (table 2, columns 1 or 2) and glass (table 2, column 6) are the only phases present.

The presence of reverse zoning in some large olivine crystals, and analyses of the bulk composition of the run demonstrate that about 30% of the original iron was lost from the sample to the $Ag_{50}Pd_{50}$ capsule. If this effect is allowed for and a mass balance is attempted using the bulk composition of column 8, table 2 it can be shown that 56% olivine (column 2), 43% glass (column 6), and 1% chromite (column 5) gives reasonable agreement for SiO_2, TiO_2, Al_2O_3, CaO and K_2O but gives high MgO and low FeO figures. Careful analysis of the outer rims of olivine crystals reveal Fe-concentrations higher than those in the glass or within the olivine crystals. Analyses of such margins, when corrected for admixture of glass by use of the Ca, Al and Ti contents, yield compositions consistent with thin borders of Fe-rich olivine (e.g. column 3, table 2) as quench outgrowth on the primary crystals. Further evidence for non-equilibrium between glass and olivine crystals is provided by data on Fe/Mg partition between olivine and liquid [21, 22] which predicts that a liquid in equilibrium with olivine (Fo_{93}) should itself have 100 Mg/(Mg + Fe^{++}) ~ 80. The analysed glass has an Mg-value of 64 (table 2). It is considered that the evidence presented establishes the presence of quench outgrowths of more Fe-rich olivine on the primary crystals, resulting from partial crystallization of the equilibrium liquid during quench cooling. The composition of the residual glass is thus not that of the equilibrium liquid.

Although it has been shown that, even in the deceptively simple run products at 10 kb and 1200°C, it is not possible to determine the composition of the partial melt directly, it remains possible to *calculate* the equilibrium liquid composition by allowing for the effects of iron loss and using the empirically determined partition coefficient between Fe/Mg in olivine and liquid [21, 22]. Residual chromite (1%) will contain most of the chromium in the charge. Knowing the equilibrium olivine composition (Fo_{93}) and bulk composition Mg-value of 89.7 after the run and the bulk composition Mg-value of 85.2 before the run, the equilibrium olivine composition, *had there been no Fe-loss*, can be calculated and is $Fo_{90.1}$ (column 4, table 2). From the Fe/Mg partition relation for olivine: liquid equilibrium [21, 22], the liquid in equilibrium with olivine of composition $Fo_{90.1}$ has 100 Mg/(Mg + Fe^{++}) = 73.5. Assuming olivine ($Fo_{90.1}$) chromite (1%) and liquid are the only equilibrium phases in the pyrolite composition at 10 kb and 1200°C, then the charge would be about 54% molten and the liquid would be of composition similar to that in table 2 (column 9) and would be classed as a magnesian, quartz-rich tholeiite (5–7% normative quartz depending on whether Fe_2O_3 = 0 or 1.5%, respectively). There is a small uncertainty in calculating 100 Mg/(Mg + Fe^{++}) of the equilibrium liquid because change in the oxidation state may occur during the run. Analyses for Fe^{++} and Fe^{+++} for runs in $Ag_{50}Pd_{50}$ capsules indicate a decrease in Fe_2O_3/FeO during runs [23]. In table 2 (column 9) the calculated 100 Mg/(Mg + Fe^{++}) value assumes no change in Fe_2O_3 content and the 100 Mg/(Mg + ΣFe) value assumes all Fe^{+++} reduced to Fe^{++}. The value for a liquid in equilibrium with $Fo_{90.1}$ is 100 Mg/(Mg + Fe^{++}) = 73.5 and lies between those values obtained using the assumptions on Fe^{+++} discussed bove.

From the data in table 2, it is inferred that a liquid produced by 32.5% melting of pyrolite (i.e. 54% melting of pyrolite minus 40% olivine) under water-saturated conditions would have a composition very similar to that of column 9, table 2, leaving residual olivine ($Fo_{90.1}$) and a trace of chromite. The liquid would be a magnesian quartz tholeiite (5–7% quartz). Since olivine is the dominant residual phase, liquids

would become less quartz-normative and then become olivine normative with higher degrees of melting.

5.1.2. 10 kb, 1100°C

Optical examination of this run resulted in identification of euhedral olivine and clinopyroxene in a glassy matrix. Tentative identification of rare tabular crystals, with straight extinction and low birefringence, as orthopyroxene [12] was not confirmed by electron microprobe examination which identified only olivine ($Fo_{89.8}$) and low alumina, chrome diopside ($Ca_{42}Mg_{52}Fe_6$). A liquid in equilibrium with olivine of this composition has 100 Mg/Mg + Fe^{++} ≃ 73 [21, 22] and this is much higher than the Mg-value of the glass (table 3). As in the 1200°C run, the composition of the glass, which is very similar to that at 10 kb and 1200°C, is considered to result from rapid metastable growth of crystalline phases during quenching. As there are two crystalline phases present, it is not possible to use the data on bulk composition, mineral composition and Mg/Fe partition between olivine and liquid, to calculate the equilibrium liquid composition without specifying the relative proportions of olivine and clinopyroxene. Optical, X-ray and microprobe examination shows that clinopyroxene is a very minor phase relative to olivine.

Analysis of the bulk composition showed slight Fe-loss, taking the Mg-value from 85.2 to 86.4. Thus the composition of the equilibrium olivine, assuming no Fe-loss, is calculated as $Fo_{89.0}$ rather than $Fo_{89.8}$ (table 3). A liquid in equilibrium with olivine ($Fo_{89.0}$) has 100 Mg/(Mg + Fe^{++}) ≃ 71 [21, 22]. In table 3, column 5, the composition of a liquid is calculated by assuming 47% melting of (pyrolite – 40% olivine) and a residual mineralogy of 49% olivine (cf. 45% at 1200°C), 1% chromite, and 3% clinopyroxene. The liquid has an Mg-value of 69.5 – 74, depending on the assumed oxidation state.

The composition of the liquid formed by partial melting of pyrolite at 10 kb 1100°C under water-saturated conditions cannot be specified uniquely by direct melting studies but the composition given in column 5 of table 3 must be a close approximation to the melt composition. It differs from the melt at 10 kb 1200°C in its higher SiO_2 content and in lower Ca/Al, lower MgO and higher TiO_2 and K_2O contents, and has 9–11% normative quartz (i.e. it may be classified as a basaltic andesite composition). Liquids of this character would be produced by ~28% partial melting of pyrolite leaving clinopyroxene-bearing dunite (olivine (Fo_{89}) + chrome diopside + accessory chromite) as residue. The absence of orthopyroxene as a residual phase for these conditions is noteworthy. Orthopyroxene would become even less

TABLE 3

	Analyzed olivine	Calculated olivine	Analyzed clinopyroxene	Glass	Calculated equilibrium liquids derived from initial composition less (49% Ol (Fo_{89}) + 1% chromite + 3% Cpx).
SiO_2	41.5	40.7	54.0	61.6	56.1
TiO_2	–	–	0.4	1.6	2.5
Al_2O_3	–	–	1.3	16.3	12.4
Fe_2O_3	–	–	–	–	1.7 } 7.3
FeO	9.8	10.7	3.6	3.7	5.8
MnO	–	–	0.1	0.1	0.1
MgO	48.2	48.5	18.8	3.2	9.3
CaO	0.2	0.1	20.5	11.2	9.5
Na_2O	–	–	0.2	>1.5	2.0
K_2O	–	–	–	0.9	0.5
Cr_2O_3	–	–	1.4	–	0.1
"H_2O"				(12.5)	
$\frac{100\ Mg}{Mg + Fe^{++}}$	89.8	89.0	?90.4	–	74
$\frac{100\ Mg}{Mg + \Sigma Fe}$	89.8	89.0	90.4	60.3	69.5

Run conditions: 10 kb, 1100°C, 1 hr, $Ag_{50}Pd_{50}$ capsule. 100 Mg/(Mg + ΣFe) of sample after run: 86.4.

important as a residual phase for water-saturated melting at lower pressures but more important at higher pressures (fig. 1). These relationships become important in seeking to interpret very magnesian dunites, wehrlites and harzburgites of the alpine-type ultramafic complexes as possible residues and accumulates from either island arc or mid-oceanic ridge magma genesis.

5.1.3. 10 kb, 1050°C

Olivine, orthopyroxene, clinopyroxene and liquid are primary phases at these run conditions. Analysis of the bulk composition shows that there has been no detectable Fe-loss (table 4). The increasing degree of crystallization of the charge is accompanied by decreasing forsterite content of olivine ($Fo_{88.5}$). The analyses of pyroxene 'pairs' at 10 kb 1020°C and 1000°C, and at 20 kb 1050°C, consistently yielded clinopyroxene with slightly higher Mg-value and slightly higher TiO_2 content than coexisting orthopyroxene. It appears probable that the analysis of clinopyroxene in the 10 kb 1050°C run includes a small proportion of quench clinopyroxene outgrowth giving slightly low Mg-value and high Al_2O_3 and TiO_2 contents (tables 4, 5, 6, 9).

The amphibole composition is that of a quench phase, on the basis of the Mg-value (too low for equilibrium with olivine or pyroxenes but probably correct for equilibrium with the glass composition), very high TiO_2 and low CaO contents and very high SiO_2 contents. In these respects the amphiboles of both the 1050°C and 1020°C runs are similar to one another and markedly different from the subsolidus amphibole at 970°C (table 7) or the amphibole (considered to be an equilibrium phase) at 1000°C (table 6). Because of the presence of quench amphibole, the Mg-value relationships between glass and crystals, and the evidence deduced

TABLE 4

	Olivine	Orthopyroxene	Clinopyroxene	Quench amphibole	Glass
SiO_2	41.2	56.6	54.0	53.1	65.0
TiO_2	–	0.2	0.8	3.8	0.9
Al_2O_3	–	1.5	3.9	13.3	21.0
FeO	11.1	7.6	4.0	6.4	2.7
MnO	–	–	–	–	–
MgO	47.5	32.4	16.3	14.8	1.5
CaO	0.15	1.3	20.1	5.4	8.7
Na_2O	–	–	0.3	$\geqslant$ 0.9	> 0.8
K_2O	–	–	–	0.6	0.6
Cr_2O_3	–	0.6	1.0	–	–
"H_2O"				(2%)	(~13.5)
$\frac{100\ Mg}{Mg + \Sigma Fe}$	88.5	88.5	88.0	80.5	51

Run conditions: 10 kb, 1050°C, 4 hr, $Ag_{75}Pd_{25}$ capsule. 100 Mg/(Mg + ΣFe) of sample after run: 85.2.

TABLE 5

	Olivine	Orthopyroxene	Clinopyroxene	Quench amphibole	Glass 1*	Glass 2*
SiO_2	40.5	55.1	53.7	53.5	56.2	64.0
TiO_2	–	0.2	0.6	2.1	3.8	0.7
Al_2O_3	–	1.1	2.0	11.0	17.7	21.0
FeO	12.3	7.6	3.8	6.4	5.9	2.4
MnO	–	–	–	–	–	–
MgO	46.8	33.8	17.7	15.3	7.4	2.5
CaO	–	1.3	21.2	8.8	6.4	8.3
Na_2O	–	–	0.2	0.3	> 1.1	> 0.7
K_2O	–	–	–	0.3	0.7	0.6
Cr_2O_3	–	0.6	0.9	0.3	0.7	–
$\frac{100\ Mg}{Mg + \Sigma Fe}$	87.2	88.8	89.3	81	69	65

Run conditions: 10 kb, 1020°C, 4 hr, $Ag_{75}Pd_{25}$ capsule. 100 Mg/(Mg + ΣFe) of sample after run: 85.3.

* Stationary electron beam giving low Na_2O value.

TABLE 6

	Olivine	Orthopyroxene	Clinopyroxene	Amphibole	Glass
SiO_2	40.5	54.5	51.5	44.6	Not
TiO_2	–	0.4	1.0	2.5	analyzable
Al_2O_3	–	4.1	4.6	11.0	
FeO	13.3	8.4	4.2	6.0	
MnO	–	–	–	0.1	
MgO	46.2	30.8	17.8	19.9	
CaO	0.1	1.1	19.5	10.9	
Na_2O	–	–	0.6	1.9	
K_2O	–	–	0.1	0.3	
Cr_2O_3	–	0.8	0.7	0.9	
$\frac{100\ Mg}{Mg + Fe}$	85.3	86.9	88.4	85.4	

Run conditions: 10 kb, 1000°C, 6 hr, $Ag_{75}Pd_{25}$ capsule.

in this and previous runs for outgrowth of quench clinopyroxene and olivine respectively, the highly siliceous glass is considered to be a non-equilibrium quench product and to bear no relation to the composition of an equilibrium melt at 10 kb 1050°C in water-saturated pyrolite composition.

It is not possible to deduce the composition of the equilibrium melt at 10 kb 1050°C without rather arbitrary assumptions about the degree of crystallization and the proportions of olivine, orthopyroxene and clinopyroxene. The decrease in Mg-value of crystalline phases between 1100°C and 1050°C implies a decrease in the amount of liquid present and the low Na and K values of the pyroxenes imply that these elements are concentrated in the liquid phase. These factors, and the increased proportion of pyroxenes (with 54–57% SiO_2) to olivine, all argue that the equilibrium liquid, with 100 Mg/(Mg + Fe^{++}) = 69–70 will have $SiO_2 < 56\%$ and high alkali contents.

5.1.4.10 kb, 1020°C

This run is similar to the 1050°C run in both the nature and compositions of its phases. Orthopyroxene ($Ca_{2.5}Mg_{86.5}Fe_{11}$) appears to be slightly high in CaO but the coexisting clinopyroxene ($Ca_{43.5}Mg_{50.5}Fe_6$) has low TiO_2, Al_2O_3 and very low Na_2O contents, and the composition is considered to be free of quench contamination. Both the amphibole and glass compositions show non-equilibrium characteristics as in the 1050°C runs, and the microprobe data, while confirming the presence of amphibole at 1020°C as observed optically [12], demonstrate that it is not an equilibrium phase at 1020°C. The glass appears to be more variable in composition in this run than in the higher temperature runs.

5.1.5. 10 kb, 1000°C

This experimental run contains olivine, orthopyroxene ($Ca_{2.2}Mg_{84.8}Fe_{13.0}$), clinopyroxene ($Ca_{41}Mg_{52}Fe_7$) and amphibole, all as major constituents and all with Mg-values consistent with the four phases being primary and in equilibrium with each other. This con-

TABLE 7

	Orhopyroxene * 1	Amphibole * 2	Orthopyroxene 3
SiO_2	53.9	44.0	54.0
TiO_2	0.4	2.1	0.2
Al_2O_3	3.7	12.0	3.3
FeO	8.9	5.6	8.9
MnO	0.2	–	–
MgO	30.5	18.1	31.2
CaO	⩽1.1	11.3	0.8
Na_2O	–	1.8	–
K_2O	–	0.5	–
Cr_2O_3	0.6	2.6	0.7
$\frac{100\ Mg}{Mg + Fe}$	86.1	85.3	86.4

Columns 1,2 – run conditions: 10 kb, 970°C, 5.5 hr, $Ag_{75}Pd_{25}$ capsule.
Column 3 – run conditions: 10 kb, 900°C, 6 hr, $Ag_{75}Pd_{25}$ capsule.

* The fine grain-size of the run product did not allow complete resolution of olivine (⩾ $Fo_{85.6}$) and clinopyroxene (⩾ 18.8% CaO) from surrounding crystals.

clusion is particularly important with respect to amphibole and derives from knowledge of compositions of co-existing amphiboles, olivine and pyroxenes in natural high-temperature ultramafic rocks [24–27]. Glass is a minor component (probably $< 10\%$) of the charge and did not occur in areas large enough for analysis. The observation that the amphibole has lower K/Na ratio than that of the subsolidus amphibole at 970°C has the corollary that the equilibrium liquid is higher in K/Na ratio than either the amphibole or the initial mix.

5.1.6. 10 kb, 970°C, and 10 kb, 900°C

Both these run products are finer grained than for higher temperature runs and satisfactory analyses (as judged) by structural formulae) were only possible for orthopyroxene and amphibole at 970°C and orthopyroxene at 900°C. Nevertheless, the increased K/Na ratio of the amphibole compared with that at 1000°C is a clear indication of some melting at 1000°C. The compositions of amphibole and orthopyroxene provide no chemical evidence for an additional melt phase at 970°C.

Comparing orthopyroxene compositions in all 10 kb experimental runs, there is a steady decrease in CaO content with decreasing temperature and it is particularly instructive to compare the 900°C orthopyroxene ($Ca_{1.7}Mg_{84.8}Fe_{13.5}$) with natural peridotite orthopyroxenes from lherzolite inclusions, high temperature peridotites, etc. Many such orthopyroxenes contain $< 0.8\%$ CaO and have equilibrated with clinopyroxene at $T < 900$°C, on the evidence presented here. The Al_2O_3 content of orthopyroxene (and of clinopyroxene) increases rather sharply at 1000°C, marking the first appearance of a relatively Al-rich coexisting phase (amphibole). At lower temperatures the Al_2O_3 content of orthopyroxene decreases whereas TiO_2 and Cr_2O_3 contents are insensitive to temperature changes within this range.

5.2. Compositions of quenched glasses and equilibrium liquids in experimental runs at 20 kb

5.2.1. 20 kb, 1100°C

Under these conditions the experimental charge showed a high degree of melting with euhedral olivine and orthopyroxene being obvious primary phases but broad plates of clinopyroxene in parallel growth to orthopyroxene showed optical characteristics indicative, in part, of quench growth. Some well-formed amphibole crystals were also optically consistent with primary crystallization. However, the chemical analyses in table 8 demonstrate that clinopyroxene was probably absent at 20 kb 1100°C, with orthopyroxene, olivine, accessory chromite and liquid being the equilibrium assemblage for water-saturated melting conditions.

Bulk analysis of the sample shows a very small Fe-loss which would only slightly affect the compositions of the residual phases. The residual olivine is Fo_{90} compared with the calculated equilibrium olivine (Fo_{89}) at 10 kb 1100°C and Fo_{90} at 10 kb 1200°C, and this implies that the degree of partial melting at 20 kb 1100°C must be about 30%. Also, since orthopyroxene is present in similar proportion to olivine, and clinopyroxene is absent, the equilibrium liquid at 20 kb 1100°C, relative to that calculated for 10 kb 1100°C (table 3), must be lower in SiO_2 and higher in CaO, Na_2O and TiO_2. Calculated compositions are given in columns 8 and 9 of table 8 and are of olivine tholeiitic character. These calculated equilibrium liquid compositions are not unique solutions because variation in percentage of melting and in the relative proportions of olivine and orthopyroxene would produce solutions also consistent with the olivine: liquid, Mg/Fe partition constraint. However, if the estimate of the degree of partial melting is increased then liquids will become quartz-normative but also have too low 100 Mg/(Mg + Fe^{++}) values for equilibrium with olivine Fo_{90}. The latter effect can be countered by decreasing the olivine proportion in the residue but his then makes the liquids increasingly olivine-normative. By reasoning of this type, it can be shown that the composition of liquid derived by partial melting of pyrolite at 20 kb 1100°C, leaving only residual olivine and orthopyroxene, must be very similar to the compositions given in columns 8 and 9 of table 8. These compositions are of olivine tholeiitic character but of lower normative olivine content than for olivine tholeiite magmas produced by melting of dry pyrolite or of pyrolite with low water content [12, 15, 21].

TABLE 8
Analyses of minerals and glasses present in (pyrolite minus 40% olivine) composition at 20 kb. The last two columns contain calculated liquid compositions compatible with equilibrium with olivine of Fo_{90} composition and derived using estimated relative proportions of residual olivine and orthopyroxene (3 : 2).

								Calculated equilibrium liquids	
	Olivine	Ortho-pyroxene	Quench * clino-pyroxene	Quench clino-pyroxene	Quench amphibole	Glass	Glass Kushiro et al. [1]	27% melting of pyrolite	30% melting of pyrolite
SiO_2	41.5	55.4	51.3	47.6	45.5	68.9	67.8	48.5	48.4
TiO_2	–	–	1.6	3.3	1.9	0.2	0.6	2.7	2.4
Al_2O_3	–	1.7	4.4	7.7	14.5	19.6	16.1	12.2	11.0
FeO	9.7	6.6	5.3	7.9	13.1	1.1	1.1	9.6††	9.4‡
MnO	–	–	–	–	0.2	–	–	0.2	0.2
MgO	48.9	33.9	16.6	13.0	11.6	0.8	0.6	11.3	14.4
CaO	–	1.3	19.2	19.5	8.9	6.1	10.2	10.7	9.6
Na_2O	–	–	0.4	0.7	2.0	$\geqslant$ 1.8 **	3.1†	2.1	1.9
K_2O	–	–	–	–	0.4	1.4	0.3	0.5	0.4
Cr_2O_3	–	1.0	1.3	0.5	–	–	–	1.1	1.0
$\frac{100\ Mg}{Mg + \Sigma Fe}$	90.0	90.0	85.0	74.5	61	58	49	68	73
$\frac{100\ Mg}{Mg + Fe^{++}}$								72	77
"H_2O"					(2%)	(~15%)			

Run conditions: 20 kb, 1100°C, 1 hr, $Ag_{75}Pd_{25}$ capsule.
Run description: Large (> 10 μ euhedral olivine and orthopyroxene. Orthopyroxene with broad clinopyroxene borders with characteristics of quench clinopyroxene (wavy extinction, RI $\gg$ Opx). Quench mica, amphibole and common glass also occur. Small brown euhedral spinel crystals are probably also primary rather than quench phases and are occasionally included in olivine and orthopyroxene. 100 Mg/Mg + ΣFe) of sample after run: 85.7.

* This is the most magnesian clinopyroxene composition analyzed but the differences in TiO_2, Al_2O_3 and 100 Mg/(Mg + ΣFe) contents between orthopyroxene and the clinopyroxene suggest that these phases are not in equilibrium with each other. It is inferred that the two clinopyroxene compositions in the table represent growth stages in quench growth of clinopyroxene. It is possible that primary clinopyroxene occurs as cores to the quench phase and is included in the analysis of the more Mg-rich clinopyroxenes but this cannot be proven on the evidence available.

** Analysis of the small areas of glass required use of a stationary beam. The Na_2O figure has been corrected by the factor found for analyses using both stationary beam (with Na volatilization) and moving beam on the 10 kb, 1200°C and 1150°C runs.

† The Na_2O figure is inferred from the bulk composition and the estimated degree of crystallization. Analysis gave low values due to Na-volatilization.

†† Calculated as 1.8% Fe_2O_3, 8.0% FeO.

‡ Calculated as 1.6% Fe_2O_3, 8.0% FeO.

5.2.2. 20 kb, 1050°C

At these conditions the primary phases are olivine, orthopyroxene and calcium-rich clinopyroxene. Quench clinopyroxene and quench amphibole are both present in the run product and the residual glass is highly siliceous and Al_2O_3-rich. Because of the presence of amphibole and quench clinopyroxene outgrowths on primary crystals and the probability that olivine is also rimmed by quench outgrowth, the composition of the glass is considered to have no similarity to the composition of the original equilibrium liquid under these conditions. The rather large change in Mg-value of olivine and orthopyroxene between 1100°C and 1050°C suggests that there is much less liquid present at 1050°C

TABLE 9

	Olivine	Ortho-pyroxene *	Clino-pyroxene *	Quench clino-pyroxene	Quench amphibole	Glass 1 **	Glass 2 **
SiO_2	40.7	53.5	53.2	45.6	47.4	70.0	68.8
TiO_2	–	0.2	0.5	3.3	2.2	0.2	0.1
Al_2O_3	0.1	2.5	2.3	9.0	15.5	19.3	21.0
FeO	12.1	8.1	4.1	8.8	10.8	0.9	0.6
MnO	–	0.1	–	–	–	–	–
MgO	46.9	33.9	17.6	17.2	11.2	1.2	0.5
CaO	0.1	1.0	20.8	14.2	8.4	5.7	7.2
Na_2O	–	–	0.4	0.8	2.0	$\geqslant 1.5$	$\geqslant 1.0$
K_2O	–	–	–	–	0.4	1.2	0.8
Cr_2O_3	–	0.9	1.1	0.2	0.1	–	–
$\frac{100\ Mg}{Mg + Fe}$	87.5	88.0	88.5	77.5	65	72	60
"H_2O"					(2%)	(16%)	(15%)

Run conditions: 20 kb, 1050°C, 4 hr, $Ag_{75}Pd_{25}$ capsule.
Run description: Large ($\geqslant 10\ \mu$) euhedral orthopyroxene, olivine and clinopyroxene as outgrowths on orthopyroxene and also as separate crystals. Primary crystals enclosed in glass with quench mica and quench amphibole. Estimated ~20% melting.
100 Mg/(Mg + ΣFe) of sample after run: 85.6.

* Note the similar 100 Mg/(Mg + Fe), Al_2O_3, TiO_2 contents of the two pyroxenes in contrast to the orthopyroxene and quench clinopyroxene of table 8.

** Glass analyses using stationary beam, Na_2O values estimated from 10 kb data evaluating the effect of Na volatilization by the electron beam.

TABLE 10

	Olivine	Orthopyroxene	Clinopyroxene	Ilmenite
SiO_2	41.4	53.9	50.8	–
TiO_2	–	0.2	0.7	59.4
Al_2O_3	0.1	4.5	6.0	0.7 *
FeO	12.7	8.0	4.1	25.0
MnO	–	–	–	–
MgO	45.2	31.6	16.3	12.1
CaO	0.2	0.9	20.6	–
Na_2O	–	–	0.6	–
K_2O	–	–	0.1	–
Cr_2O_3	–	0.9	0.8	2.4
NiO	0.4	–	–	–
$\frac{100\ Mg}{Mg + Fe}$	86.4	87.6	87.8	46.3

Run conditions: 20 kb, 1000°C, 4 hr, $Ag_{75}Pd_{25}$ capsule.
Run description: Common olivine and orthopyroxene laths and minor clinopyroxene in quench amphibole + mica + glass. Accessory ilmenite and spinel included in some orthopyroxene and olivine. Differs from the 1100°C run in the absence of *broad* clinopyroxene borders on the orthopyroxene laths.

* Al_2O_3 may be too high from matrix interference.

TABLE 11

	Olivine	Orthopyroxene	Clinopyroxene
SiO_2	40.2	53.2	51.0
TiO_2	–	0.3	0.6
Al_2O_3	–	5.5	5.0
FeO	12.6	8.5	4.4
MnO	–	–	–
MgO	46.7	30.3	16.8
CaO	–	1.0	20.8
Na_2O	–	0.1	0.6
K_2O	–	–	0.1
Cr_2O_3	–	0.7	0.8
NiO	0.4	–	–
$\frac{100\ Mg}{Mg + Fe}$	86.9	86.5	87.3

Run conditions: 20 kb, 970°C, 6 hr, $Ag_{75}Pd_{25}$ capsule. Run description: Common orthopyroxene, olivine and clinopyroxene (commonly as simply-twinned crystals) together with mica (possibly primary) and spinel (and ilmenite) and minor interstitial glass.

TABLE 12

	Olivine	Ortho-pyroxene	Clino-pyroxene	Amphibole
SiO_2	40.5	53.2	51.3	44.3
TiO_2	–	0.4	0.3	1.1
Al_2O_3	–	5.4	4.6	13.6
FeO	13.9	8.8	3.8	5.5
MnO	–	–	–	–
MgO	45.1	30.5	17.0	19.1
CaO	0.1	0.8	21.2	10.4
Na_2O	–	–	0.7	2.4
K_2O	–	–	–	0.5
Cr_2O_3	–	0.7	1.0	1.1
NiO	0.4	–	–	–
$\frac{100\ Mg}{Mg + Fe}$	85.2	86.1	88.9	86.1

Run conditions: 20 kb, 950°C, 6 hr, $Ag_{75}Pd_{25}$ capsule. Run description: Common olivine, orthopyroxene, amphibole (small colourless laths), minor clinopyroxene and accessory ilmenite and spinel. No evidence for melting, orthopyroxene does not have borders of (quench) clinopyroxene.

than at 1100°C, and the low Na_2O, K_2O and TiO_2 contents of the primary clinopyroxene shows that the liquid will be enriched in these elements while retaining $SiO_2 < 50\%$ (because of the increasing importance of pyroxenes as residual phases).

5.2.3. 20 kb, 1000°C, 970°C and 950°C

In these runs, although quench phases and glass were present at 1000°C and 970°C, only primary phases have been analyzed. With decreasing temperature the Mg-values of olivine and orthopyroxene * decrease, with the compositions at 950°C being similar to those at 970°C and 900°C (both subsolidus) at 10 kb. The presence of Mg, Cr-rich ilmenite at 1000°C is noteworthy. This phase is probably present, though not analyzable, in lower temperature runs and would account for the lower TiO_2 content of amphibole at 20 kb 950°C than that at 10 kb 970°C and 10 kb 1000°C. In comparing the subsolidus, primary amphibole at 950°C with quench amphibole at 1050°C and 1100°C the main difference is in Mg-value in CaO, TiO_2 and SiO_2 contents. The K_2O/Na_2O ratio of the amphibole at 950°C is lower than that of the starting mix and this effect is more marked when the Na_2O content (0.7%) of the clinopyroxene is also considered . This comparison suggests the presence of a minor K-rich phase, possibly phlogopite or a trace of K-rich melt phase. If a melt phase is present and thus 950°C is slightly above the solidus, then the amount of melt must be too small to affect Mg-values.

The analysis of coexisting pyroxene pairs in these runs shows a similar temperature dependence of the width of the pyroxene miscibility gap at both 10 kb and 20 kb. There is some suggestion that orthopyroxene shows slightly lower CaO content at a given temperature at 20 kb than at 10 kb. The data at 950°C 20 kb support the view that orthopyroxene-clinopyroxene pairs in lherzolites, in which orthopyroxene has $< 0.8\%$ CaO and clinopyroxene has $> 20\%$ CaO, have equilibrated at $T < 1000$°C.

6. Application of the experimental melting studies to models of the upper mantle

6.1. The lithosphere and low velocity zone

The experimental data presented in this paper provide constraints on both geophysical and petrogenetic

* Because of its readiness to form inclusion-free porphyroblasts or phenocrysts, orthopyroxene is the most easily analysed mineral in the assemblage and thus the best for noting changes in Mg-value, Al_2O_3 content etc..

aspects of the upper mantle. Firstly, the determination of the pyrolite solidus in the presence of small amounts of water (water-undersaturated, p_{H_2O} determined by equilibrium between pargasitic amphibole and its breakdown products) establishes a firm petrological model for the low velocity zone (LVZ) of the upper mantle. If the water content of the upper mantle is $< 0.4\%$ approximately, the petrological model predicts a relatively stable location of the roof to the low velocity zone at depths equivalent to 27–29 kb load pressure (85–95 km approx.) due to intersection of the local geothermal gradient with the pyrolite solidus. Variation in the local geothermal gradient would cause variation in the degree of partial melting (and thus the magnitude of the seismic attenuation) within the LVZ and possibly considerable variation in the depth to the floor of the LVZ, with little change in the depth to the roof of the LVZ (base of the lithosphere). The data on subsolidus mineralogy for (pyrolite + 0.2% H_2O) also show that the appearance of garnet would occur along an oceanic geotherm at load pressures of approximately 17–19 kb (55–66 km). This mineralogical change would cause a small increase in density and possibly in seismic velocity in the lower part of the lithosphere; similar mineralogical zoning for an anhydrous mantle has been discussed previously [5, 6].

The data illustrating the position of the pyrolite solidus for water-saturated melting show that the base of the lithosphere, if located by the intersection of the geotherm with the pyrolite solidus, may move abruptly from depths of 85–95 km to depths of 60–70 km, without change in the local geothermal gradient, *if* the water content of the lower part of the lithosphere is increased to exceed $\sim 0.4\%$ H_2O. Addition of water to previously immobile lithosphere may occur from underthrust lithosphere of a subduction zone, and may lead to rather high degrees of partial melting and mantle diapirism from depths of 60–70 km, the degree of partial melting increasing as the diapirs moved towards the surface.

The experimental data provide an explicit model for two different tectonic regimes (fig. 3). The water-undersaturated melting data are applied to yield a model of a relatively stable lithosphere and LVZ, either in oceanic or continental regions, in which volcanism may occur either by simple fracturing of the lithosphere and direct tapping of the small melt fraction in the LVZ, or by tensional thinning of the lithosphere with

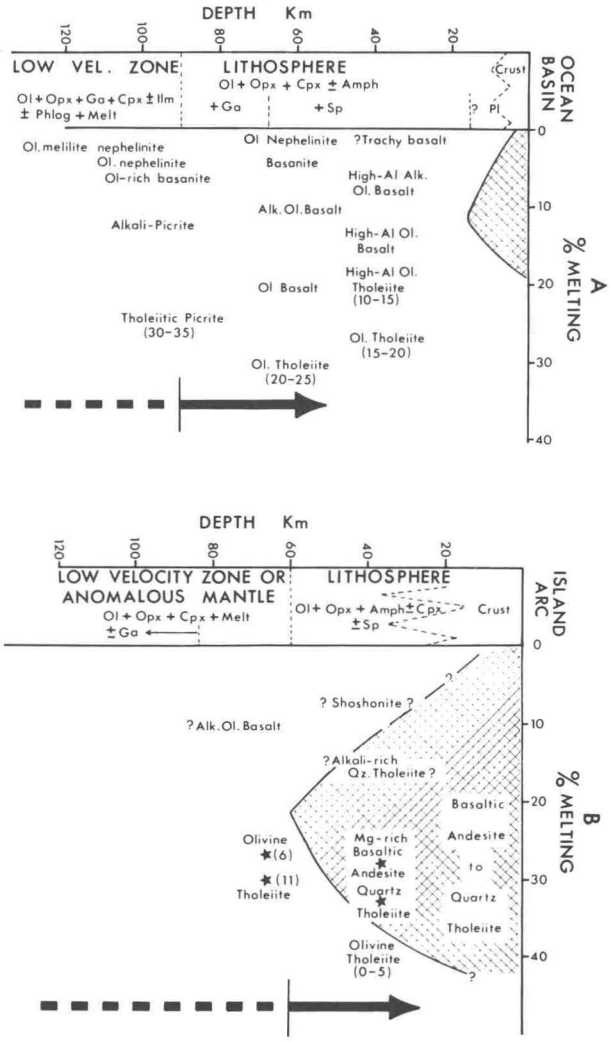

Fig. 3. Diagram summarizing the petrogenetic applications of the melting studies on pyrolite composition. The column to the left illustrates the mineralogical character of the lithosphere and depth to the onset of partial melting in the island arc situation and the normal oceanic crust-mantle situation. In the right side of the diagrams, the character of magma derived by partial melting of pyrolite is plotted as a function of depth of magma segregation and degree of partial melting. Numbers in parentheses adjacent to basalt names refer to the normative olivine content of the partial melt. The hatched areas illustrate the range of conditions over which *quartz-normative* magmas may be derived by direct partial melting and magma segregation from pyrolite. (A) is compiled for melting under water-undersaturated conditions, with a water content in the source pyrolite of about 0.2%. (B) is compiled for melting under water-saturated conditions. The asterisks denote the specific liquid compositions calculated at 10 kb and 20 kb in this paper.

consequent upwelling and diapirism from the LVZ leading to higher degrees of partial melting and shallower depths of magma segregation. If the latter process develops into large-scale rifting apart of lithospheric plates, then the deeper parts of the LVZ become involved in the upwelling at the rift axis and act as major magma sources. The data of fig. 2 may in this way, be applied to quantify the specific models of basaltic volcanism of mid-oceanic ridge, rift valley, island chain and oceanic island situations which were developed previously [12, 15–17].

In contrast to this tectonic setting, the data on water-saturated melting is applied to yield a model of an unstable situation in which the base of the lithosphere moves to depths of 60–70 km due to access of water (to exceed about 0.4% H_2O) and the higher water contents produce higher degrees of partial melting at depths $>$ 60 km. This setting is one in which mantle diapirism, in some cases from reactivated lithosphere, would lead to high degrees of melting under water-saturated or near-saturated conditions and to magma segregation at rather shallow depths. The tectonic conditions described would occur if there were access of proportionately large amounts of water to the upper 60–150 km of the mantle. Such conditions may occur in the wedge of mantle overlying the Benioff zone in oceanic trench-island arc situations where the source of proportionately large and rapidly released amounts of water can be attributed to dehydration reactions in subducted lithosphere [2, 3, 12, 13, 18, 20].

6.2. *Magma genesis in island arcs*

As well as defining the P, T conditions of melting of a pyrolite upper mantle under water-saturated conditions, the data presented establish the nature of the magmas produced by partial melting under these conditions. It has been shown that with sufficiently high degrees of melting of pyrolite at 10 kb such that olivine (+ accessory chromite) is the only residual phase ($\sim$ 32% melting), the melt is of magnesian quartz tholeiite character. For lower degrees of melting (28%) of pyrolite under these conditions, liquids with $\sim$10% normative quartz and $\sim$56% SiO_2 are produced at temperatures of $\sim$ 1100°C, leaving residual wehrlite (olivine + clinopyroxene ± accessory chromite). For $<$ 25% melting, at 10 kb and $T < 1100$°C, the magma composition cannot as yet be clearly specified but the evidence presented suggests that liquids will have higher alkali-content but retain SiO_2 contents of around 55%. Magmas such as the highly magnesian, low-calcium, quartz-rich "andesites" (56–58% SiO_2) of Cape Vogel, Papua [28, 31] might be products of high degrees of melting of pyrolite under water-saturated conditions with magma segregation occurring at $<$ 10 kb [29].

The data presented in this paper on the experimental melting of pyrolite show that water-saturated, magnesian quartz tholeiites and basaltic andesites may be derived by direct partial melting of *pyrolite* at $\sim$ 10 kb but that water-saturated olivine tholeiites are the least undersaturated magmas which may be derived by partial melting of pyrolite at $\sim$20 kb. These conclusions support those of Nicholls and Ringwood [2, 3] who have carried out the necessary complementary study, i.e. the determination of the liquidus phases of olivine tholeiite, quartz tholeiite and basaltic andesite under water-saturated conditions. These studies [2, 3] defined the expansion of the field of olivine as a liquidus phase in quartz-normative natural rock compositions under water-saturated conditions and demonstrated that such liquids could be equilibrium melt products of a peridotite source, leaving residual olivine. The data presented in this paper do not support the conclusion that andesitic or dacitic magmas can be derived by direct partial melting of peridotite at pressures up to 25 or 30 kb [1,7–9, 29]. More importantly, the data provide clear evidence that the presence of highly siliceous glasses in quenched high-pressure runs containing a large proportion of primary crystals (either with or without readily identifiable quench phases) is a result of metastable fractionation of liquid during quenching, caused by the outgrowth of rims on primary phases and/or nucleation of quench clinopyroxene, amphibole and mica. The compositions of such glasses are not consistent with equilibrium between liquid and primary olivine and pyroxenes of the peridotite source rock and do not constitute evidence for the genesis of siliceous ($>$ 55% SiO_2) liquids by partial melting of peridotite under water-saturated conditions at $P > 10$ kb.

Acknowledgements

The author acknowledges the skill and assistance of W.O. Hibberson in carrying out the experimental runs. The installation and calibration of the TPD electron probe by S.J.B. Reed and N.G. Ware has added greatly to the usefulness of this technique in experimental petrology. The critical comments of I.A. Nicholls, A.E. Ringwood and T.H. Green on the manuscript, particularly in areas where the present study integrates with their own experiments, resulted in improvements to the data (role of Fe-loss, particularly) and to the manuscript. The comments of the reviewers for the manuscript have materially improved the paper. These contributions are gratefully acknowledged.

References

[1] I. Kushiro, N. Shimizu and Y. Nakamura, Compositions of coexisting liquid and solid phases formed upon melting of natural garnet and spinel lherzolites at high pressures: A preliminary report, Earth Planet. Sci. Letters 14 (1972) 19.

[2] I.A. Nicholls and A.E. Ringwood, Production of silica-saturated tholeiitic magmas in island arcs, Earth Planet. Sci. Letters (in press).

[3] I.A. Nicholls and A.E. Ringwood, Effect of water on olivine stability in tholeiites and the production of silica-saturated magmas in the island arc environment (submitted for publication).

[4] A.E. Ringwood, Composition and evolution of the upper mantle, in: The earth's crust and upper mantle, P.J. Hart ed., Amer. Geophys. Union Monograph 13 (1969) 1.

[5] D.H. Green and A.E. Ringwood, The stability fields of aluminous pyroxene peridotite and garnet peridotite and their relevance in upper mantle structure, Earth Planet. Sci. Letters 3 (1967) 151.

[6] D.H. Green and A.E. Ringwood, Mineralogy of peridotitic compositions under upper mantle conditions, Phys. Earth Planet. Interiors 3 (1970) 359.

[7] I. Kushiro, Y. Syono and S. Akimoto, Melting of a peridotite nodule at high pressures and high water pressures, J. Geophys. Res. 73 (1968) 6023.

[8] H.S. Yoder, Calc-alkali andesites: Experimental data bearing on the origin of their assumed characteristics, Oregon Dept. Geol. Mineral. Ind. Bull. 65 (1969) 77.

[9] I. Kushiro, Systems bearing on melting of the upper mantle under hydrous conditions, Carnegie Inst. Washington Year Book 68 (1970) 240.

[10] L.A. Fontijn, A.B. Bok and J.G. Kornet, The TPD electron probe X-ray Micro-Analyzer in: 5th Internat. Congress on X-ray Optics and Micro-Analysis, G. Mollenstedt and K.H. Gaukler, eds. (1969) p. 261.

[11] D.H. Green, Conditions of melting of basanite magma from garnet peridotite, Earth Planet. Sci. Letters 17 (1973) 456.

[12] D.H. Green, Magmatic activity as the major process in the chemical evolution of the earth's crust and upper mantle, Tectonophysics 13 (1972) 47.

[13] D.H. Green, Contrasted melting relations in a pyrolite upper mantle under mid-oceanic ridge, stable crust and island arc environments, Tectonophysics (in press).

[14] I.B. Lambert and P.J. Wyllie, Stability of hornblende and a model for the low velocity zone, Nature 219 (1968) 1240.

[15] D.H. Green, The origin of basaltic and nephelinitic magmas, Trans. Leicester Literary and Philosophical Soc. 64 (1970) 28.

[16] A.E. Ringwood, The chemical composition and origin of the earth, in: Advances in earth science, P.M. Hurley ed. (M.I.T. Press, Cambridge Mass., 1966) p. 287–356.

[17] D.H. Green, Compositions of basaltic magmas as indicators of conditions of origin: Application to oceanic volcanism, Phil. Trans. Roy. Soc. A 268 (1970) 707.

[18] P. Jakes and J.B. Gill, Rare earth elements and the island arc tholeiitic series, Earth Planet. Sci. Letters 9 (1970) 17.

[19] P.J. Wyllie, Role of water in magma generation and initiation of diapiric uprise in the mantle, J. Geophys. Res. 76 (1972) 1328.

[20] P. Jakes and A.J.R. White, Major and trace element abundances in volcanic rocks of orogenic areas, Geol. Soc. Amer. Bull. 83 (1972) 29.

[21] D.H. Green and A.E. Ringwood, The genesis of basaltic magmas, Contr. Mineral. Petrol. 15 (1967) 103.

[22] P.L. Roeder and R.F. Emslie, Olivine-liquid equilibrium, Centr. Mineral. Petrol. 29 (1970) 275.

[23] A.J. Irving, Geochemical and high pressure experimental studies of xenoliths, megacrysts and basalts from S.E. Australia, unpublished Ph. D. thesis, Australian Nat. Univ., Canberra (1971).

[24] D.H. Green, The petrogenesis of the high-temperature peridotite in the Lizard area, Cornwall J. Petrol. 5 (1964) 134.

[25] D.B. MacKenzie, High temperature alpine-type peridotite from Venezuela, Geol. Soc. Amer. Bull. 71 (1960) 303.

[26] F. Frey and D.H. Green, The geochemistry and origin of lherzolite inclusions in Victorian basanites (in preparation).

[27] R. Varne, Hornblende lherzolite and the upper mantle, Contr. Mineral. Petrol. 27 (1970) 45.

[28] W.B. Dallwitz, D.H. Green and J.E. Thompson, Clinoenstatite in a volcanic rock from the Cape Vogel area Papua, J. Petrol. 7 (1966) 375.

[29] I. Kushiro, Effect of water on the composition of magmas formed at high pressures, J. Petrol. 13 (1972) 311.

[30] S.J.B. Reed and N.G. Ware, Quantitative electron microprobe analysis using a lithium-drifted silicon detecton (submitted for publication, 1972).

[31] W.B. Dallwitz, Chemical composition and genesis of clinoenstatite-bearing volcanic rocks from Cape Vogel, Papua: A discussion in: Proc. 23rd Internat. Geol. Congress 2 (1968) 229.